Yttrium oxyhydrides for photochromic applications: Correlating composition and optical response

Dmitrii Moldarev,[1,2] Marcos V. Moro,[1] Chang C. You,[3] Elbruz M. Baba,[3,4] Smagul Zh. Karazhanov,[2,3] Max Wolff,[1,2,*] and Daniel Primetzhofer[1]

[1]*Department of Physics and Astronomy, Uppsala University, Box 516, 751 20 Uppsala, Sweden*

[2]*Department of Materials Science, National Research Nuclear University (MEPhI), 115409 Kashirskoe shosse 31, Moscow, Russia*

[3]*Department for Solar Energy, Institute for Energy Technology, NO-2027 Kjeller, Norway*

[4]*Nano Science and Nano Engineering Department, Istanbul Technical University, 34469 Istanbul, Turkey*

(Received 31 August 2018; published 26 November 2018)

It has been recently demonstrated that yttrium oxyhydride (YHO) films can exhibit reversible photochromic properties when exposed to illumination at ambient conditions. This switchable optical property enables their utilization in many technological applications, such as smart windows, sensors, goggles, and medical devices. However, how the composition of the films affects their optical properties is not fully clear and therefore demands an investigation. In this paper, the composition of YHO films manufactured by reactive magnetron sputtering under different conditions is deduced in a ternary diagram from time-of-flight elastic recoil detection analysis. The results suggest that stable compounds are formed with a specific chemical formula—$YH_{2-\delta}O_{\delta}$. In addition, optical and electrical properties of the films are investigated, and a correlation with their compositions is established. The corresponding photochromic response is found in a specific oxygen concentration range ($0.45 < \delta < 1.5$) with maximum and minimum of magnitude on the lower and higher border, respectively.

DOI: 10.1103/PhysRevMaterials.2.115203

I. INTRODUCTION

Yttrium, lanthanum, and some other transition and rare-earth metals can form hydrides (e.g., YH_x and LaH_x) that exhibit a metal-to-insulator transition under hydrogenation [1]. This transition is commonly accompanied by switchable optical properties, which make such metal hydrides very attractive for applications, such as smart windows [2] and hydrogen sensors [3]. However, the implementation of smart windows based on metal hydrides requires a hydrogen-storage layer and ion transport layer to change the hydrogen concentration in the metal. In addition, an optical sensor is needed to provide a signal and allow the change of the optical properties according to the intensity of the incident light. On the other hand, materials with photoinduced switching of the optical properties allow the development of passive devices, without the need for any extra layers or sensors.

Films of YH_x exhibit a photoinduced metal to insulator transition at low temperature (<10 K) [4] and photochromism at a pressure of several gigapascals [5]. Mongstad *et al.* were the first to report on the rapid changes of optical and electrical properties of YHO upon visible and ultraviolet light illumination at ambient conditions [6]. Later, similar properties were observed in rare-earth metal oxyhydrides such as Gd, Er, and Dy [7]. Although these materials attract considerable attention of the scientific community due to their possible technological applications, the mechanisms responsible for their photochromic behavior are still poorly understood.

Positron annihilation results of YHO suggest that UV light causes either a generation of a small concentration of cation vacancies or an assembling of vacancies into vacancy clusters [8]. These observed structural changes were irreversible during the bleaching process, and therefore cannot be the reason for the reversible change in color. Nuclear magnetic resonance has indicated that YHO films in an initially transparent state contain three hydrogen species with different mobility, of which the most mobile one stays trapped under illumination and is released thereafter in the relaxation process [9]. In addition, a reversible lattice contraction under illumination was observed by time-resolved x-ray diffraction (XRD), suggesting structural changes that might be associated with the photochromism [10]. A recent study by Montero *et al.* based on optical ellipsometry and Raman spectroscopy proposed the mechanism for the photochromic effect: the illumination leads to the formation of small metallic opaque domains in the transparent insulating matrix [11]. It is hypothesized that the size of these domains is smaller than the wavelength of the visible light; thus, the YHO films become homogeneously darker. However, there is no direct evidence of domain formation yet. Other recently reported studies show that the modification of the deposition parameters causes significant changes in the composition of films, accompanied by a varying photochromic response [12,13]. Thus, a systematic study of the correlation of film composition with optical properties of the material might help to gain a more complete understanding of the photochromic behavior of YHO films.

In this paper, we present a systematic analysis of the composition of YHO films with different concentrations of H and O, using time-of-flight elastic recoil detection analysis (TOF-ERDA) as a quantitative tool yielding direct signals of all constituent species. Our results suggest a chemical formula

*max.wolff@physics.uu.se

of $YH_{2-\delta}O_\delta$ for all the films investigated, indicating that the oxygen atoms replace hydrogen in the dihydride lattice when oxidized after deposition. Additionally, combining the information of the YHO composition with *in situ* optical measurements, we establish the phase diagram for the ternary compound and the full correlation between composition and photochromic response.

II. RESULTS AND DISCUSSION

For all samples described in Table I, TOF-ERDA spectra reveal the main constituents yttrium, hydrogen, and oxygen, even though the films were deposited in an oxygen-free atmosphere. Light trace impurities (such as C, N, and F) were detected as well, however their respective concentration is found to be ≈1–2 at. % constant throughout the films for the investigated samples. Recent findings suggest that the oxygen present in the films enters after the deposition during exposure to the atmosphere [14]. Additionally, an oxygen-enriched surface layer has been reported from combined Rutherford backscattering spectrometry and neutron reflectometry studies [15]. A thin surface oxide, as well as impurities of light elements, are expected for composites of transition and rare-earth metals, due to their high chemical reactivity. Besides the oxygen-enriched layer on the surface, all elements are uniformly distributed throughout the film. Thermal annealing of the films at temperatures above 100 °C leads to strong oxidation accompanied by hydrogen release as shown in Fig. 1. Moreover, the films oxidize uniformly, indicating a high mobility of the oxygen and hydrogen atoms in the YHO.

TABLE I. Deposition conditions and annealing parameters of the YHO films investigated in this paper.

Notation	Type	Transparency	Annealing temperature (°C)	Annealing time (min)
GI-1	Gradient	Transparent		
GI-2	Gradient	Transparent		
GI-3	Gradient	Transparent		
GI-4	Gradient	Opaque		
GI-5	Gradient	Opaque		
GII-1	Gradient	Transparent	150	45
GII-2	Gradient	Transparent	150	45
GII-3	Gradient	Transparent	150	45
GII-4	Gradient	Transparent	150	45
GII-5	Gradient	Opaque	150	45
GII-6	Gradient	Opaque	150	45
GII-7	Gradient	Opaque	150	45
GIII-1	Gradient	Transparent	215	45
GIII-2	Gradient	Transparent	215	45
GIII-3	Gradient	Transparent	215	45
GIII-4	Gradient	Transparent	215	45
GIII-5	Gradient	Transparent	215	45
GIII-6	Gradient	Opaque	215	45
HI	Homogeneous	Transparent	50	30
HII	Homogeneous	Transparent	110	30
HIII	Homogeneous	Transparent	165	30
HIV	Homogeneous	Transparent	200	30

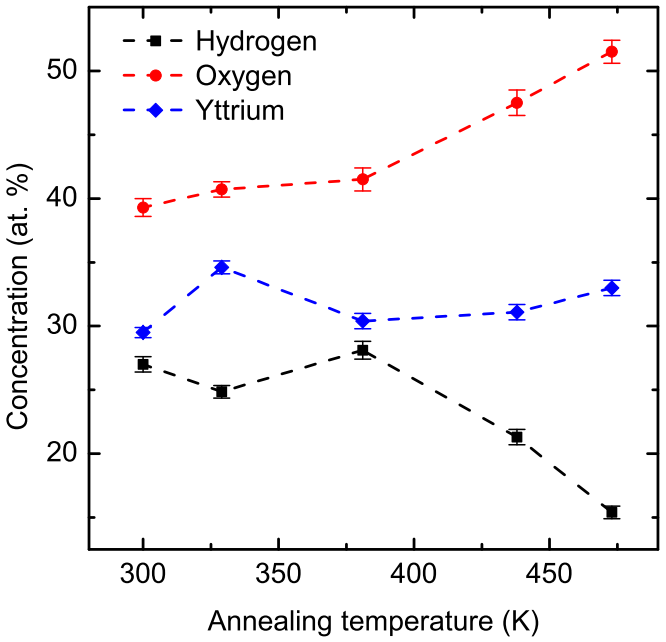

FIG. 1. Composition deduced from TOF-ERDA of the homogeneous sample after 30 min of annealing at different temperatures.

The ternary diagram of Y, H, and O in Fig. 2 illustrates the composition deduced for the samples investigated in this paper. Red triangles and blue diamonds represent the transparent and opaque films, respectively. The Y, H, and O concentrations shown in Fig. 2 are depth-integrated values (in atomic percent), not including the thin oxygen-enriched layer at the surface. The concentration of oxygen and hydrogen strongly changes from one sample to another, whereas the yttrium amount only slightly fluctuates around 33 at. %. This result suggests the YHO films are oxidized yttrium dihydride with a chemical formula of $YH_{2-\delta}O_\delta$. Here, δ represents the

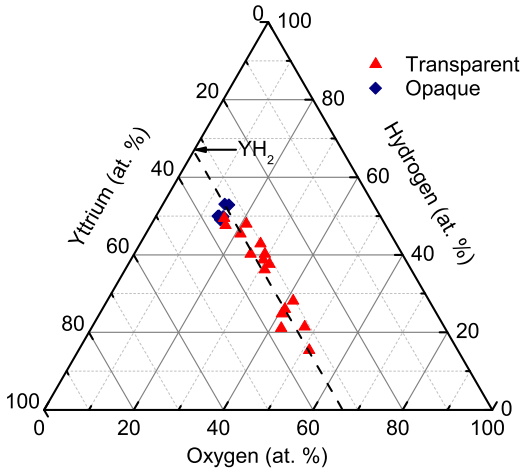

FIG. 2. Composition as deduced from TOF-ERDA and represented in a ternary diagram of Y, H, and O. Red triangles and blue diamonds mark transparent and opaque films, respectively. The dashed line represents compositions corresponding to the chemical formula $YH_{2-\delta}O_\delta$ suggested in this paper, whereas the black arrow shows the composition for pure YH_2.

number of oxygen atoms per yttrium atom. This findings implies that oxygen atoms replace hydrogen in the film during the oxidation process. It was reported that similar films have an fcc structure corresponding to the YH_2 phase with a slightly expanded lattice due to the oxygen atoms [10,16]. This observation is in agreement with the proposed general formula. According to the definition [17], the oxidation states of the main constituents are yttrium 3+, oxygen 2−, and hydrogen 1−. Therefore, the only value of δ that would fulfill the charge neutrality condition is 1, which corresponds to the $Y^{3+}H^{-}O^{2-}$ compound. However, for most of the samples, it was found that δ significantly deviates from unity. In case of $\delta < 1$, charge neutrality can be reached if Y possesses mixed oxidation state 2+ and 3+, whereas the formation of a neutral compound with $\delta > 1$ (for instance $\delta > 1.55$ for the sample HIV) is possible, if H and O bond with each other creating OH^{-} complexes, in accordance with Ref. [18].

It should be noted that the diagram corresponds to the condition when the $YH_{2\pm\delta}$ has been oxidized in air at room temperature and ambient pressure. However, if oxidation has been performed at different conditions and in different atmospheres (e.g., water vapor, ozone, hydrogen peroxide, or containing aldehydes, formaldehydes, alcohols, or organic acids), lattices, phases, and compositions of Y-H-O different from those in Fig. 2 might be formed.

You *et al.* reported that films of YHO prepared at different deposition conditions show a different photochromic response [19]. The optical properties of the films were studied and correlated with the composition. In Fig. 3 the transmission coefficient (averaged over wavelength from 500 to 900 nm) and the direct optical band gap for all samples investigated in this paper are shown in Figs. 3(a) and 3(b), respectively, as a function of oxygen to yttrium ratio (i.e., δ). At a low oxygen concentration (i.e., $\delta \approx 0.4$), the films are opaque and metallic, like pure YH_2. However, at a critical concentration δ_{critical} (horizontal dotted line in Fig. 3), the transmittance rapidly increases up to 55%, whereas further oxidation leads to a smooth increase of the transmittance up to 88% at $\delta = 1.6$ [Fig. 3(a)]. The change of transmittance is followed by a change of the band gap [Fig. 3(b)]: the films become semiconducting with $E_g = 2.8$ eV when the oxygen concentration exceeds δ_{critical}. Further, a band gap widening up to 3.8 eV is observed with increasing δ. Since the transmittance and band gap of yttrium oxyhydride vary depending on oxygen concentration, it should be possible to alter both transparency and color if the dihydride film is oxidized in a controlled way. The critical oxygen concentration δ_{critical} apparently corresponds to a metal-to-semiconductor phase transition and is estimated to be 0.45 ± 0.05.

In order to study the photochromic properties of the YHO films, optical transmittance spectra before and under illumination were measured. The results for the sample GI-2 are shown in Fig. 4(a), which is representative for all samples with photochromic behavior. After 30 min of illumination, the initial transmittance of the film of ≈70% is reduced homogeneously in a wavelength range above the absorption edge (≈450 nm). No midgap states have been formed that filter the visible light. This property is one of the advantages of YHO films compared to other inorganic oxide-based photochromic films [20]. Figure 4(b) presents time-resolved reducing and bleaching

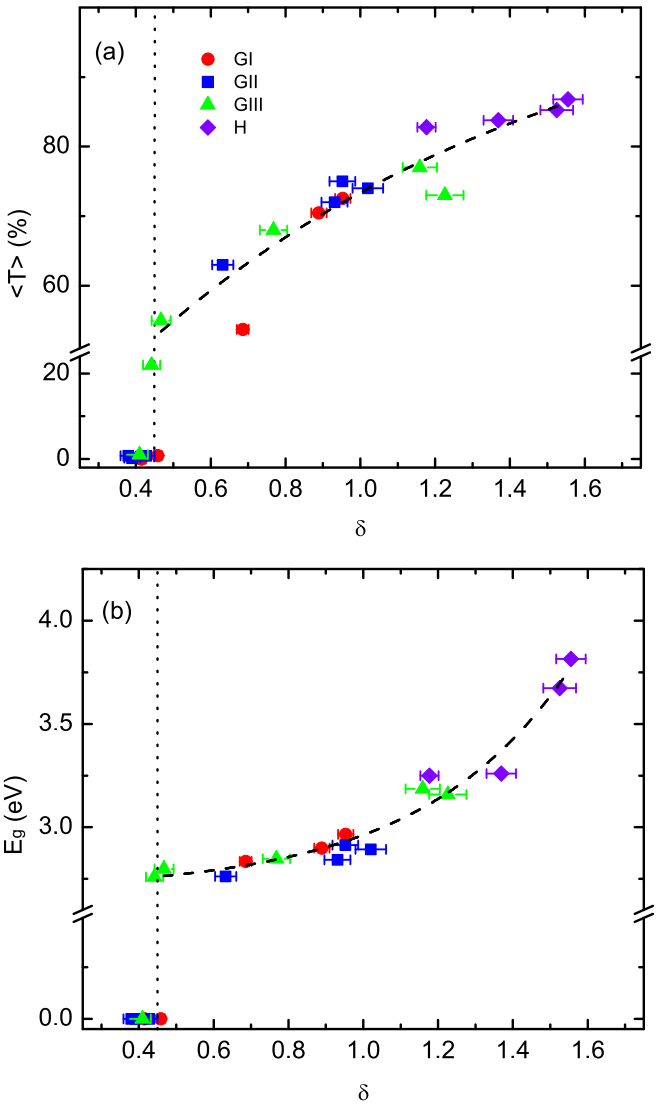

FIG. 3. Transmission coefficient (averaged over 500–900 nm) (a) and direct optical band gap (b) plotted as a function of the oxygen to yttrium ratio δ. The dashed lines represent the fit to the data using an exponential decay and growth for transmittance and band gap, respectively. The dotted lines show the threshold value of δ where the transition from the metallic opaque to the insulator transparent state is observed.

of the average transmittance over a wavelength range from 500 to 900 nm under illumination by blue laser light ($\lambda = 375$ nm). The fastest change of transmission is found during the first few minutes followed by a slower photodarkening. Similar dynamics are observed during bleaching of the film when the laser is switched off. Even though the dynamics of both processes resemble an exponential behavior, a single exponential cannot fit them.

Figure 5 shows the magnitude of the observed photochromic response of the YHO films after 30 min of illumination, as a function of composition. Three different areas (i.e., phases) can be identified in terms of the photochromic response. The first phase is associated with slightly oxidized dihydride at $\delta < 0.45$ and exhibits properties similar to pure YH_2: it is a metallic and opaque material, which does not

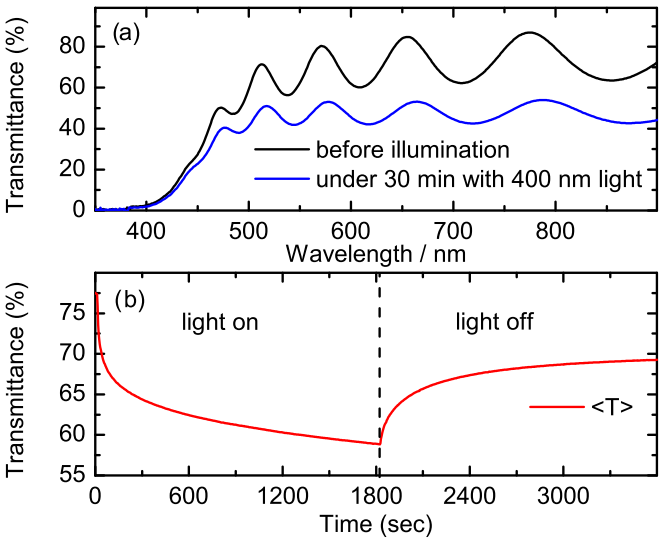

FIG. 4. Transmission spectra (a) of the sample GI-2 measured before illumination and after 30 min of illumination. Time-resolved changing of the transmittance (b) under blue laser ($\lambda = 375$ nm) illumination and bleaching.

exhibit a detectable photochromic effect. The second phase, in the range $0.45 < \delta < 1.5$, represents a transparent-yellowish semiconductor exhibiting photochromism. The magnitude of the photochromic response, however, strongly depends on the oxygen concentration: a clear maximum is observed at low oxygen concentrations and the effect gradually decreases with increasing the oxygen concentration and almost vanishes at the upper boundary. Finally, the third phase, which forms at a high oxygen concentration $\delta > 1.5$, is an almost fully transparent semiconductor, which does not show any pronounced photodarkening because the photons incident on the film are not absorbed by the material with band gap exceeding the

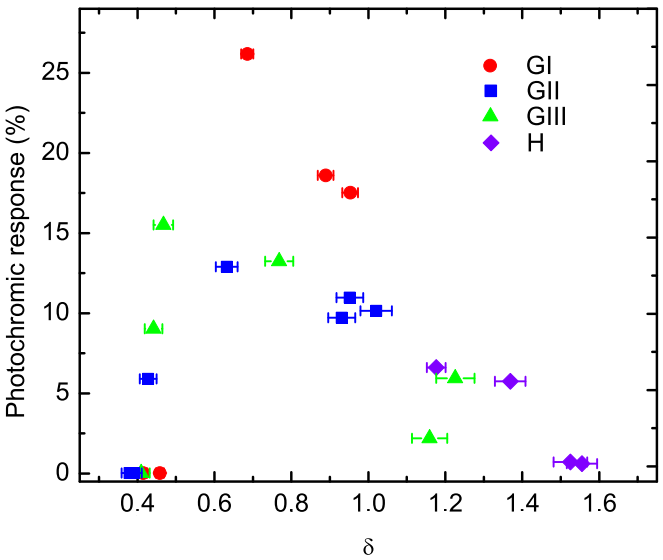

FIG. 5. Photochromic response (averaged from 600–800 nm) after 30 min of blue laser ($\lambda = 375$ nm) illumination plotted as a function of the oxygen to yttrium ratio, δ.

photon energy. Nevertheless, XRD experiment showed all phases having a similar crystalline structure resembling YH_2 (225 space group), but with a different lattice parameter.

According to the transmittance results, at $\delta = 0.45$ the films undergo a metal-to-semiconductor transition. The reason for the presence or lack of a photochromic behavior of the YHO films—below and above $\delta = 1.5$—might also be connected to the interplay of the band-gap value and the incident photon energy. In the present paper, a blue laser with 3.3 eV photon energy was used. At $\delta > 1.5$ the band gap of the films exceeds 3.3 eV [see Fig. 3(b)] so incoming photons are not able to excite electrons. Thus, the border between transparent photochromic and transparent nonphotochromic phases at $\delta = 1.5$ may be rather conditional and dependent on the wavelength of light illuminating the film.

III. SUMMARY AND CONCLUSIONS

In this paper, we present a systematic composition analysis of YHO. The results reveal that oxygen replaces hydrogen during the oxidation processes, hence a formal chemical formula is suggested: $YH_{2-\delta}O_\delta$. This findings indicates that $YH_{2-\delta}O_\delta$ belongs to the emerging class of materials called oxyhydrides with mixed oxide, hydride, and hydroxide anions sharing the same sites in the lattice. Although building construction, medicine, and sensors are considered as the possible applications of $YH_{2-\delta}O_\delta$, the interest is broader than this. The ternary diagram is plotted and the dependence of the optical properties on composition is established for oxidation in air, at room temperature and ambient pressures. From the optical studies, we establish a correlation between transmittance and photochromic response to the composition of the films: slight oxidation (i.e., $\delta < 0.45$) does not cause significant changes and the films properties are similar to pure YH_2. When the concentration of oxygen exceeds δ_{critical}, a metal-to-semiconductor transition takes place and they become transparent with a band gap of >2.6 eV. Further oxidation induces a gradual increase of transmittance and band-gap widening. *In situ* measurements of transmittance under illumination have revealed that yttrium oxyhydride exhibits photochromic behavior in the range $0.45 < \delta < 1.5$. The strength of the photochromic response is found to decrease with increasing oxygen concentration in the film accompanied by an optical band-gap widening. Finally, our results demonstrate that controlled postoxidation of metal hydride thin films provides the opportunity to produce photochromic coatings with tailored switchable optical and electrical properties, interesting for energy-saving smart windows and other applications.

IV. EXPERIMENTAL SECTION

YHO films were deposited onto transparent glass substrates by reactive magnetron sputtering in mixed Ar and H_2 atmosphere using a Leybold Optics A550V7 on-axis pulsed in-line dc magnetron sputtering machine. Two different sets of samples were produced: samples with a color gradient in the lateral direction from black opaque to yellowish and yellowish transparent and with homogeneous optical properties. For the latter one, the H_2:Ar gas ratio was kept constant at 0.21. In order to achieve homogenous transparency of the film, the

sample carrier oscillated in front of the yttrium target during deposition. The gradient samples were deposited with 200-sccm gas flow, and 0.25 H_2:Ar gas ratio. The typical thickness of the films, measured by profilometry, is around 800 nm. Further information on the sample preparation procedures, as well as illustrative photos of the gradient samples, can be found elsewhere (see, for instance, Fig. 1 in Ref. [13]). After the growth, twins of the samples were annealed at different temperatures under ambient pressure in order to study the oxidation process as well as to diversify the composition. In total, seven samples were used in this paper: three gradient and four homogeneous ones. The composition and the optical response of the gradient samples were measured on several spots. All samples are summarized in Table I with respect to their type (gradient or homogeneous), deposition conditions, and annealing parameters.

The optical characterization of the YHO films was investigated using a Perkin Elmer Lambda 35 UV/Vis spectrophotometer, equipped with tungsten and deuterium light sources. The transmission measurements were calibrated with respect to 100% transmission in air. Tauc plots were used to extract the optical band gap [21]. In order to trigger the photochromic reaction in the films, the samples were illuminated for 30 min using a lamp with monochromatic light at ≈400−nm wavelength. Time-resolved transmittance measurements were performed under blue laser illumination with a 375-nm wavelength. XRD measurements were performed using a Philips PW3020 diffractometer equipped with an x-ray tube with Cu anode.

The composition analysis of the films was carried out by TOF-ERDA. This ion-beam technique enables us to obtain depth profiles of chemical elements. In this paper, TOF-ERDA was performed at the 5 MV pelletron tandem accelerator at Uppsala University, delivering 36 MeV $^{127}I^{8+}$ as probe beam. The samples were mounted with the sample normal positioned under 67.5° with respect to the incident beam. The TOF telescope tube is fixed at 45° with respect to the direct beam. During the measurements, gradient samples were scanned along its gradient axis. Further details on the TOF-ERDA setup at Uppsala University employed in this paper can be found in Ref. [22].

Two software packages were used to obtain depth profiles from the experimental TOF-ERDA spectra: CONTES [23] and Potku [24]. Both provide identical results on the stoichiometry within the statistical uncertainties of the experiment, which is $\leqslant 2\%$ for the deduced Y, O, and H concentrations in all samples. Other systematic uncertainties, resulting from, e.g., inaccuracies of the energy loss of the primary ions and recoil species, are estimated on the order of 5–10%. However, the relative concentration of the elements is determined with higher accuracy (see supplements in Ref. [25]).

ACKNOWLEDGMENTS

The authors would like to acknowledge the Visby Programme Scholarships for Ph.D studies and the Carl Trygger foundation for financial support. Support by Swedish research council (Contracts No. 821-2012-5144 and No. 2017-00646_9) and the Swedish Foundation for Strategic Research (Contract No. RIF14-0053) supporting accelerator operation are also gratefully acknowledged. The work by the IFE group has received financial support from the Research Council of Norway through FRINATEK Project No. 240477/F20 and from the internal project "Yttrium smart window" at Institute for Energy Technology S-40073.

[1] J. N. Huiberts, R. Griessen, J. H. Rector, R. J. Wijngaarden, J. P. Dekker, D. G. de Groot, and N. J. Koeman, Nature (London) **380**, 231 (1996).

[2] K. Yoshimura, C. Langhammer, and B. Dam, MRS Bull. **38**, 495 (2013).

[3] A. L. Stepanov, A. Reinholdt, and U. Kreibig, in *Nanotechnological Basis for Advanced Sensors*, edited by J. P. Reithmaier, P. Paunovi, W. Kulisch, C. Popov, and P. Petkov (Springer, Berlin, 2011), Chap. 39, pp. 381–389.

[4] A. F. T. Hoekstra, A. S. Roy, T. F. Rosenbaum, R. Griessen, R. J. Wijngaarden, and N. J. Koeman, Phys. Rev. Lett. **86**, 5349 (2001).

[5] A. Ohmura, A. Machida, T. Watanuki, K. Aoki, S. Nakano, and K. Takemura, Appl. Phys. Lett. **91**, 151904 (2007).

[6] T. Mongstad, C. Platzer-Björkman, J. P. Maehlen, L. P. A. Mooij, Y. Pivak, B. Dam, E. S. Marstein, B. C. Hauback, and S. Zh. Karazhanov, Sol. Energy Mater. Sol. Cells **95**, 3596 (2011).

[7] F. Nafezarefi, H. Schreuders, B. Dam, and S. Cornelius, Appl. Phys. Lett. **111**, 103903 (2017).

[8] M. P. Plokker, S. W. H. Eijt, F. Naziris, H. Schut, F. Nafezarefi, H. Schreuders, S. Cornelius, and B. Dam, Sol. Energy Mater. Sol. Cells **177**, 97 (2018).

[9] C. V. Chandran, H. Schreuders, B. Dam, J. W. G. Janssen, J. Bart, A. P. M. Kentgens, and P. J. M. van Bentum, J. Phys. Chem. C **118**, 22935 (2014).

[10] J. P. Maehlen, T. T. Mongstad, C. C. You, and S. Zh. Karazhanov, J. Alloys Compd. **580**, S119 (2013).

[11] J. Montero, F. A. Martinsen, M. García-Tecedor, S. Z. Karazhanov, D. Maestre, B. Hauback, and E. S. Marstein, Phys. Rev. B **95**, 201301(R) (2017).

[12] D. Moldarev, D. Primetzhofer, C. C. You, S. Z. Karazhanov, J. Montero, F. Martinsen, T. Mongstad, E. S. Marstein, and M. Wolff, Sol. Energy Mater. Sol. Cells **177**, 66 (2018).

[13] C. C. You, D. Moldarev, T. Mongstad, D. Primetzhofer, M. Wolff, E. S. Marstein, and S. Zh. Karazhanov, Sol. Energy Mater. Sol. Cells **166**, 185 (2017).

[14] J. Montero, F. A. Martinsen, M. Lelis, S. Zh. Karazhanov, B. C. Hauback, and E. S. Marstein, Sol. Energy Mater. Sol. Cells **177**, 106 (2018).

[15] T. Mongstad, C. Platzer-Björkman, J. P. Mæhlen, B. C. Hauback, S. Zh. Karazhanov, and F. Cousin, Appl. Phys. Lett. **100**, 191604 (2012).

[16] T. Mongstad, C. Platzer-Björkman, S. Zh. Karazhanov, A. Holt, J. P. Maehlen, and B. C. Hauback, J. Alloys Compd. **509**, S812 (2011).
[17] P. Karen, P. McArdle, and J. Takats, Pure Appl. Chem. **88**, 831 (2016).
[18] T. Mongstad, A. Thøgersen, A. Subrahmanyam, and S. Zh. Karazhanov, Sol. Energy Mater. Sol. Cells **128**, 270 (2014).
[19] C. C. You, T. Mongstad, J. P. Maehlen, and S. Zh. Karazhanov, Appl. Phys. Lett. **105**, 31910 (2014).
[20] Y. Shigesato, Jpn. J. Appl. Phys. **30**, 1457 (1991).
[21] J. Tauc, R. Grigorovici, and A. Vancu, Phys. Status Solidi **15**, 627 (1966).
[22] P. Ström, P. Petersson, M. Rubel, and G. Possnert, Rev. Sci. Instrum. **87**, 103303 (2016).
[23] M. S. Janson, CONTES conversion of time-energy spectra: A program for ERDA data analysis, Uppsala University Internal Manual, 2004 (unpublished).
[24] K. Arstila, J. Julin, M. I. Laitinen, J. Aalto, T. Konu, S. Kärkkäinen, S. Rahkonen, M. Raunio, J. Itkonen, J.-P. Santanen, T. Tuovinen, and T. Sajavaara, Nucl. Instrum. Methods Phys. Res. Sect. B: Beam Interact. with Mater. Atoms **331**, 34 (2014).
[25] M. A. Arvizu, R.-T. Wen, D. Primetzhofer, J. E. Klemberg-Sapieha, L. Martinu, G. A. Niklasson, and C. G. Granqvist, ACS Appl. Mater. Interfaces **7**, 26387 (2015).